TO DETERMINE THE FATE OF PACKAGED HISTONES DURING HPV16 VIRAL INFECTION

by

Nianyu Chi

A Thesis Submitted to the Faculty of the

DEPARTMENT OF CELLULAR AND MOLECULAR MEDICINE

In Partial Fulfillment of the Requirements

For the Degree of

MASTER OF SCIENCE

In the Graduate College

THE UNIVERSITY OF ARIZONA

2023

THE UNIVERSITY OF ARIZONA
GRADUATE COLLEGE

As members of the Master's Committee, we certify that we have read the thesis prepared by **Nianyu Chi**, titled **To determine the fate of packaged histones during HPV16 viral infection** and recommend that it be accepted as fulfilling the dissertation requirement for the Master's Degree.

Samuel Campos (Jul 17, 2023 10:19 PDT)

Samuel Campos, Ph.D. Date: Jul 17, 2023

Lonnie Lybarger, Ph.D. Date: Jul 17, 2023

Ritu Pandey (Jul 17, 2023 11:39 PDT)

Ritu Pandey, Ph.D. Date: Jul 17, 2023

Final approval and acceptance of this thesis is contingent upon the candidate's submission of the final copies of the thesis to the Graduate College.

I hereby certify that I have read this thesis prepared under my direction and recommend that it be accepted as fulfilling the Master's requirement.

Samuel Campos

Samuel Campos, Ph.D. Date: Jul 17, 2023
Master's Thesis Committee Chair

Acknowledgements

I would like to thank my mentor, Dr. Samuel Campos, for his support and patience.

I would also like to acknowledge Dr. Samuel Campos, Dr. Lonnie Lybarger, and Dr. Ritu Pandey for their guidance and help.

I would also thank the following people in Dr. Campos's lab for their kind help. Dr. Shuaizhi Li, Isabelle Toby, Matthew Christofferson, Zach Williamson, Advait Jeevanandam.

Table of contents

List of figures

Abstract

High-risk human papillomaviruses (HPVs) cause 5% of all human cancer worldwide. HPV infects mucosal and cutaneous epithelia and induces cellular proliferation. The HPV capsid, which is involved with the initial binding, internalization, and intracellular trafficking, is composed of 72 pentamers of major capsid protein L1 and up to 72 copies of minor capsid protein L2. HPV packages its genome with host histones to form a chromatin-like structure, and the viral genome acquires specific histone modifications from the host cell in which it was replicated and packaged into progeny virions. The L2 protein, complexed with the vDNA, traffics from endosomes to the trans-Golgi network (TGN), eventually arriving at the nucleus, in a trafficking process highly dependent on mitosis. En route to the nucleus, the packaged histones likely remain associated with vDNA, however, the specific details and fate of these packaged viral histones remain poorly characterized. We have produced epitope-tagged core histone pseudoviruses (PsVs) and utilized immunofluorescence microscopy to detect the transport of histones during HPV16 infection. We find that tagged histones associate with L1 protein and accumulate at the late endosome at 8h post-infection, similar to the behavior of tagged L2. Furthermore, both tagged histones and tagged L2 accumulate at nuclear PML bodies at late times post-infection. These data suggest that histones may remain coupled the L2/vDNA complex throughout the retrograde trafficking to the nucleus, and therefore have potential to carry epigenetic marks that may affect viral gene expression upon the next round of infection.

Key words: HPV16, viral histones, L2/vDNA complex, retrograde trafficking

Introduction

General background of Human Papillomaviruses

Currently, more than 200 identified genotypes of human papillomaviruses have been identified. HPVs are the most common sexually transmitted infection. The disease-associated HPVs are categorized into low-risk and high-risk types. Most low-risk HPV types (HPV6 and 11) rarely develop neoplasia or cancer but cause mucosal or cutaneous warts. The high-risk HPV types (HPV16, 18, 31, 33, 45, 52, and 58) lead to the majority of cervical cancer, and other anogenital, and oropharyngeal cancers[1], [2]. HPV 16 and HPV 18 are the most common high-risk HPV types that contribute to approximately 70% of cervical cancers in the world[3]. Papillomaviruses (PVs) are non-enveloped icosahedral dsDNA viruses that infect and replicate in different vertebrate animals including humans, other mammals, birds, reptiles, amphibian, and some fish[4], [5]. The virion capsid is composed of 360 copies of major capsid protein L1, arranged as 72 pentamers, and 72 copies of minor capsid protein L2, which interact with L1 pentamers. These two capsid proteins encapsidate an ~8kb circular, histone-associated, double-stranded DNA[6] (Fig 1A). The packaged genome (vDNA) is associated with host core histones (H2a, H2b, H3, H4), in a chromatin-like structure[7].

Infection and pathogenesis of HPV16

HPVs are classified into five evolutionary groups- they have different epithelial tropisms and different disease associations[1], [8]. HPV16 belongs to the alpha type 9, with the majority of infections occurring in the mucosal epithelium of the oral cavity and reproductive tracts, and these infections have potential to progress into oropharyngeal, anal, or cervical cancers[1]. HPV16 infects basal keratinocytes of differentiating epithelium. In the case of cervical infections, infection is believed to occur by virions

passing through micro-abrasions in the transitional zone at the junction of the endo- and ecto-cervix[9]. During viral infection, the viral genome is maintained as low copy number episomes in basal keratinocytes. As the basal cells divide and are pushed upwards into the superbasal layers, the infected cells express the E6 and E7 viral oncogenes which promote entry into S-phase, cellular DNA replication, and uncontrolled cellular division[10]. Episomal viral genomes are amplified and packaged into progeny virions within the upper squamous layer, where infectious HPV virions are release as the dead squames are shed off the host. Due to the abnormal cellular replication, the infected epithelial tissue has potential to progress into cervical cancer[11] (Fig 1B).

Although the precise mechanisms of HPV oncogenesis are not fully understood, the expressions of two early viral proteins, E6 and E7, play a critical and necessary role in causing HPV-related cancer disease[12]. E6 and E7 proteins have negative regulatory functions on the cell cycle. E6 protein not only degrade the tumor suppressor protein p53 but also activates telomerase[13], [14]. E7 protein associates with the tumor suppressor protein pRb causing release of E2F transcription factors that promote entry into S-phase of the cell cycle[15].

Viral histone modifications regulate the biological consequences of infection

Viral epigenetics play a critical role in the control of viral life cycle, infectivity, and transformation of host cells. Histones are known to affect epigenetic regulation either through the presence of different histone variants or by post-translational modification of histones[16], [17]. Histone modification, such as methylation, acetylation, phosphorylation, modulate the chromatin structure and alter between transcriptional activation and repression to regulate gene expression[18].

Histone modifications have been shown to be important in viral gene expression and viral infection. Previous studies on adenoviruses suggested that modification of histone-like proteins VII and V regulate viral protein synthesis during infection[19]. Histone-like protein VII significantly affects the phosphorylated H2AX and ATM, which are markers of DNA damage response, indicating that inhibits DNA damage response signaling on the infected cell[20]. Also, histone-like protein VII causes linker histone H1 depletion and recruitment of high mobility group box (HMGB), leading to aberrant cell cycle progression[21]. Virions of both papillomavirus families and polyomavirus families have been known to associate with host histones to form a chromatin-like structure[7], [22] (Fig 1C). An early study on polyomavirus SV40 suggested that correlation between the variations in histone modification in the SV40 chromatin and subsequent effects on an infection and related to the SV40 life cycle. For instance, the specific modified histones in epigenomes are likely associated with the repression of early transcription present at late times[23]. Also, histone acetylation has been shown to contribute towards infectivity of SV40[24]. Prior research has described that HPV vDNA acquires specific histone modification upon packaging. Intriguingly, HPV1 virions isolated from natural warts showed different histone H3 and H4 tail modification profiles compared to host chromatin from primary human foreskin keratinocyte (HFK) control cells, suggesting that wart-derived HPV1 viruses may preferentially package histones with certain modifications[25].

Subcellular trafficking of HPV16

In order for packaged histones or epigenetic marks to matter for infection, the packaged histones must stay associated with the vDNA during trafficking. The initial infection of HPV16 starts by interaction of virion with heparan sulfate proteoglycans (HSPGs), which are present on the basal keratinocytes[26]. Interaction of HSPGs with HPV16 induces

conformational changes in both L1 and L2 capsid proteins in which cell surface kallekrein-8 (KLK8) and furin cleavage occur, respectively[27], [28]. Several studies suggest annexin A2 heterotetramer, alpha 6 integrin, growth factor receptor tyrosine kinases, and tetraspanin CD151 may interact with HPV16 particles to form an entry complex[29]–[32].

L1 capsid proteins are cleaved and disassembled during trafficking through the endosomal pathway. Within late endosome/ multivesicular bodies (MVBs), L1 capsid proteins segregate away from L2/vDNA complex and are eventually degraded[33]. A conserved furin cleavage site ^{9}RTKR^{12} in L2 is cleaved by cellular furin and this step is required for endocytosis and subcellular trafficking of the L2/vDNA complex[34]. Once furin cleavage occurs, L2 capsid protein conformation changes to form the protrusion structure and acts as an inducible transmembrane protein to help vDNA traffic to the trans-Golgi network (TGN)[35] (Fig 1D).

Several other factors are required for proper HPV16 trafficking. First of all, low pH is a requirement for HPV infection[36]. Endosomal acidification seems to be required to release L2 protein and allow L2 protein to expose its transmembrane domain, membrane destabilization peptide, and retromer binding site. It was suggested that the membrane destabilization peptide aided the insertion of L2 within the acidic endosomes and displayed strong membrane-disrupting activity[37]. Previous research in our laboratory identified a glycine-rich transmembrane domain (TMD) that is utilized for L2 membrane spanning [38], [39]. Moreover, γ-secretase (γ-sec) is required for L2 membrane spanning during HPV infection. Inhibition of γ-sec or knockdown of any of the subunits of γ-sec results in a failure of L2 protrusion and L2/vDNA failed to traffic to the TGN and accumulate in endosomes[40]. Last but not least, furin cleavage plays an important part

in HPV infection. Furin cleavage somehow enables the L2 protein to insert into the membrane, although the structural basis for this is not understood. Mutation of the furin cleavage site or inhibition of furin blocks HPV infection and L2 membrane spanning [41]. Upon cellular entry into mitosis, the TGN naturally becomes fragmented and vesiculated, enabling L2/vDNA trafficking to the sister chromosome via microtubules from the minus end to the plus end, and then vDNA tether on the host chromosome and replicate with the host chromosome[35] (Fig 1E).

Purpose of the dissertation

L2 capsid proteins associate and transport the viral genome through the endosomal pathway to the TGN and to the nucleus[42]. However, little is known about whether host histones stay associated with the viral genome throughout the whole trafficking and if viral histones epigenetically regulate HPV viral gene expression during early infection. We hypothesize that viral histones are associated with L2/vDNA complex throughout the retrograde trafficking to the nucleus. We studied these core histones during viral infection by producing tagged L2 and tagged core histones HPV virions and investigating the process of infection by immunofluorescence microscopy and infection assays.

Material and methods

Cell culture

All the cell lines were maintained at 37°C with 5% CO_2. HaCaT cells (immortalized keratinocytes) were cultured in high-glucose Dulbecco's modified Eagle's medium (DMEM; 11965-092; Gibco) supplemented with 10% fetal bovine serum (FBS; A31606-02; Gibco) and antibiotic-antimycotic (Ab/Am; 15240062; Thermo Fisher Scientific). 293TT cells were grown in high-glucose DMEM with 10% FBS, Ab/Am, and hygromycin B (Fisher Scientific MT30230CR). Cell passage was performed when the cell confluence was around 80%. 0.05% trypsin-EDTA (Gibco, Life Technologies) was used for detaching adherent cells, then was neutralized by cDMEM. For cell counting, 100ul Trypan blue solution 0.4% (w/v) in PBS (Corning) and 20ul suspended cells were mixed into microfuge tubes; and then mixed solution were applied to hemocytometer for counting.

Pseudovirus production

Pseudoviruses(PsV) were generated by using 293TT cells based on experiments. Briefly, 293TT cells were $CaCl_2$ co-transfected with appropriate tagged or non-tagged viral capsid proteins pXULL based plasmids (15μg), and the luciferase reporter plasmid pGL3(15μg), plus or minus tagged viral core histone pCIP based plasmid (15μg). Changing fresh cDMEM before transfection. DNA crystal solution was prepared by diluting pXULL based plasmid, pCIP based plasmid, and pGL3 plasmid into double-distilled water and 2M $CaCl_2$ solution, then mixing with an equal volume of 2X HBS (HEPES, buffered saline, 50mM HEPES, 280mM NaCl, 1.5mM Na2PO4. Bio5 Institute Media Facility). Then, adding same volume of DNA crystal solution into each plate. Fresh cDMEM was changed on the following day. Transfected cells were harvested at 48h post-transfection.

Cells were pelleted and resuspended in PBS with 9.5mM MgCl2. Cells were lysed by 0.35% Brij58 (Bio5 Institute Media Facility) that make virus release. 1/40 volume of 1M ammonium sulfate (pH=9.0, Bio5 Institute Media Facility) was added to provide a basis environment to allow viral maturation. Then, Benzonase nuclease (Sigma e1014-25ku) was added to 0.3% final concentration and Plasmid-Safe ATP-dependent DNase (Lucigen e3101k) was added to around 20 U/ml final concentration for digesting unpackaged DNA of cells. Lysates were incubated at 37°C for 20-24h before being chilled on ice for 10 minutes and then added 0.17 volume of 5M NaCl. Lysates were frozen and thawed at -80 and 37°C one time for further CsCl purification. Viruses were purified by CsCl gradient. After centrifuged, supernatants were collected and loaded into the top of the CsCl gradient (4ml heavy (1.4g/ml) CsCl in the bottom and 4ml light (1.25g/ml) CsCl on the top). Samples were centrifuged at 20,000 rpm at 18°C for 16-24h in a Beckman SW40Ti swinging bucket rotor by using ultracentrifuge. Needles and syringes were used for collect viral bands. 100kDa MWCO Vivaspin tubes were washed and concentrated viruses by VSB (Viral Storage Buffer, 25mM HEPES with 500mM NaCl and 1mM MgCl2, PH=7.5, Bio5 Institute Media Facility). Viral bands were transferred to vivaspin tubes and centrifuged to remove the CsCl. After 3 times washing step, viruses were concentrated and collected to 100-200ul of VSB. Finally, aliquot viruses to 20ul of each and stored at -80°C. Conduct nanodrop analysis to confirm DNA concentration, then conversion to ng L1 to apply SDS-PAGE and Coomassie staining to verify the L1/L2 content in purified viruses; also, the content of the pGL3 in purified viruses was measured by SYBR green qPCR (specific primers for the luciferase gene in pGL3).

Western blots

Samples were lysed in 1X RIPA lysis buffer (50mM tris-HCl PH=8.0, 150mM NaCl, 0.5

Na-deoxycholate, 0.5% SDS. Bio5 Institute Media Facility) supplemented with 1% PMSF and 1% Proteinase inhibitor cocktail, and mixed with 20% total volume of reducing SDS-PAGE loading buffer (contain 0.5M Tris, glycerol, 10%SDS, 2-mercaptoethanol and 1% bromophenol blue) for reducing PAGE. Then, samples were incubated at 95°C for 5 minutes. 20-30ul of samples were loaded in 10% polyacrylamide gels. Gels were run at 110V in running buffer (1X Tris-Glycine-SDS. Bio5 Institute Media Facility) for 90 minutes. Next, samples on the gel were transferred onto a 0.45 μm nitrocellulose membrane using transfer buffer (0.25M Tris, 1.92M Glycine. Bio5 Institute Media Facility) with 10% methanol at 300mA for 75 minutes for blotting. Membranes were blocked in 5% non-fat powered milk dissolved in Tris-buffered saline containing 0.1% Tween (TBST) (200mM Tris, 1.5M NaCl, 1% Tween20, pH=7.5. Bio5 Institute Media Facility) at room temperature for 1 h.

For primary antibodies, Rabbit anti-GAPDH (Cell Signaling 2118S) antibody was used at 1:5,000 dilution, Mouse anti-HiBit (Promega CS2006A01) antibody was used at 1:1000 dilution, and Rat anti-HA (Roche 11867423001) antibody was used at 1:1,000 in 1% milk/TBST for staining tagged L2 and tagged histone.

For secondary antibodies, goat anti-rabbit DyLight 800 antibody, goat anti-mouse DyLight 680 antibody, goat anti-rat DyLight 800 antibodies (Fisher Scientific PISA510024) were diluted 1:10,000 in 5% milk/TBST. Membranes were imaged on the Licor Odyssey Infrared Imaging System.

Coomassie staining

For reducing PAGE, samples were lysed in 1X RIPA lysis buffer supplemented with 1% PMSF and 1% Proteinase inhibitor cocktail, and mixed with 20% total volume of reducing SDS-PAGE loading buffer. Then, samples were incubated at 95°C for 5 minutes.

20-30ul of samples were loaded in 10% polyacrylamide gels. Gels were run at 110V in running buffer for 90 minutes. Then, samples on the gel were rinsed with ddH2O for 10 minutes and then rinsed with ddH2O twice. Gel was stained with Coomassie blue for 2 h at room temperature. After incubation, gel was washed with ddH2O for 10 minutes and then rinsed with ddH2O twice. Gel was destained with destain solution at room temperature overnight. Rinsed with ddH2O twice then gels were imaged on the Licor Odyssey Infrared Imaging System.

Real-time PCR

Viral samples were mixed with 250ng proteinase K (Fermentas EO0491) supplemented with ddH2O supplemented with 50ng/ul sssDNA and incubated at 50°C for 1h and then at 95°C for 30 min. Next, added ddH2O supplemented with 50ng/ul sssDNA, NEB buffer, and pGL3 restriction enzyme (BglII) to each sample. Samples were incubated at 37°C for 1h and then at 95°C for 30 min. Then, samples were diluted to 1:5000 using ddH2O supplemented w/ 50ng/ul sssDNA. Samples were mixed with SYBR green master mix (Fisher Scientific FERK0252) with primers qLuc2-A (ACGATTTTGTGCCAGAGTCC), and qLuc2-B (TATGAGGCAGAGCGACACC) for pGL3 (final dilution:1:1000) and examined by using QuantStudio 6 Flex and data was acquired and analyzed by using QuantStudio 6 Flex Real-Time PCR System Software for measuring pseudogenome content.

Infection assay

HaCaT were plated at 50,000 cells per well in a 24-well plate. The following day, HaCaT were infected with WT(HPV16), 3XFTHA tagged L2, 3XFTHA tagged core histones at 2 x 10^8 viral genomes/well. At 24 hours post-infection (p.i.), the cells were washed once

with PBS and lysed in 100 µl reporter lysis buffer (Promega E397A) at room temperature for 10 min and then transferred to -80°C for at least 30 minutes. Samples were then thawed on ice. 20 µl of lysates were added into 96 well white microplates and mixed with 100ul of luciferase assay reagent (Promega E4550). Luciferase activity was measured on a DTX-800 multimode plate reader (Beckman Coulter). Luciferase activity normalized by BCA assay.

Immunofluorescence and Confocal microscopy

For infections, HaCaT cells were seeded on glass coverslips in 24-well plates at 50,000 cells per well. The following day, the cells were infected with 1000ng L1/ml of tagged L2 and tagged histones virus for 8 h. For colocalization with late endosome, cells were infected with tagged L2 and tagged histones PsVs at 700ng L1/ml for 8 h. Then, the cells were washed with pH7.4 PBS three times. The cells were fixed with 2% paraformaldehyde/PBS for 10 min at room temperature and permeabilized with 0.2% Triton X-100/PBS for 10 min at room temperature. The cells were blocked in 4% BSA/1% goat serum/PBS overnight at 4°C.

For colocalization with nuclear PML bodies at late times post-infection, HaCaT cells were seeded on glass coverslips in 24-well plates at 50,000 cells per well and were infected with 3XFTHA-tagged L2 and 3XFTHA-tagged histones PsVs at 700ng L1/ml with or without 200nM Compound E for 18h. Then, medium was replaced, and cells were cultured for extra 24h. At 42 h post-infection, the cells were washed with pH7.4 PBS three times, and then fixed with 100% methanol (Fisher A452SK4) at -20°C for 5 min. The cells were blocked in 4% BSA/1% goat serum/PBS overnight at 4°C.

Rabbit anti- HPV16 polyclonal antibody, raised against intact HPV16 PsV (a kind gift from the Ozbun laboratory), mouse anti-FLAG M2 antibody (Sigma F1804), rat anti-HA antibody (Roche 11867423001), mouse anti-CD63 antibody (Sigma SAB4700215), mouse anti-PML antibody (Abcam 96051) were used at 1:500 dilution. Cells were incubated with primary antibody at room temperature for 1h, followed by wash with pH7.4 PBS three times than 1h room temperature incubation of secondary Alexa Fluor 488/568 goat anti-mouse antibody, Alexa Fluor 488 donkey anti-rat antibody, and Alexa Fluor 568/647 goat anti-rabbit antibody (Molecular Probes) were used at 1:1,000 dilution.

All antibodies were diluted into PBS contain 20% blocking solution. DAPI was dilute to 1:1000 with PBS. Cells were incubated with DAPI for 1.5 minutes. Then, wash with PBS once. Prolong diamond anti-fade mounting medium (Life Tech P36970) were used for mounting coverslips. All immunofluorescence samples were collected by using Zeiss LSM880 inverted confocal microscopy. 405 nm, 488 nm, and 561 nm lasers were used to scan the samples. Images were manufactured using Zeiss LSM image software, and were processed by image J. Colocalization analysis (Manders coefficients M2) utilizing the JACoP plugin of ImageJ.

Lipofectamine 2000 transfection

293TT cells were plated at 90,000 cells per well in a 24-well plate. The following day, gently mixed the pGL3 plasmid and the pCIP-based tagged histone plasmid DNA (0.5ug/well) and Lipofectamine 2000 (Life Tech 11668019) in serum-free Opti-MEM (Life Tech 31985070). After 15 min incubation at room temperature, the plasmid DNA and Lipofectamine 2000 in Opti-MEM were combined and formed DNA-Lipofectamine 2000 complexes. The DNA-Lipofectamine 2000 complexes added to each well

containing cells and fresh cDMEM. After 6hr incubation at 37°C, the cell medium was changed with fresh cDMEM, then incubated at 37°C for an additional 24 hr.

Luciferase assay

At 24 hours post-transfection (p.i.), the 293TT cells were gently washed once with PBS and lysed in 100 µl reporter lysis buffer (Promega E397A) at room temperature for 10 min and then transferred to -80°C for at least 30 minutes. Samples were then thawed on ice. 20 µl of lysates were added into 96 well white microplates and mixed with 100ul of luciferase assay reagent (Promega E4550). Luciferase activity was measured on a DTX-800 multimode plate reader (Beckman Coulter). Luciferase activity normalized by BCA assay and checked tagged histone expression by western blot.

Results

Characterization of 3XFTHA-tagged histone viruses.

Pseudovirus is a useful approach for studying HPV *in vitro*. This is accomplished by transfection of multiple plasmids, encoding capsid protein L1/L2, luciferase reporter gene, and expression plasmids encoding epitope-tagged histones into 293TT cells to produce HPV-like viral particles that package tagged histones and contain the pGL3 plasmid encoding the luciferase reporter gene to create packaged viral particles that contain histones. These plasmids are packaged into viral particles in a size-selective manner, and only the small pGL3 reporter plasmid can be packaged efficiently (Fig 2A). In order to investigate whether host histones are associated with the L2/vDNA complex, we generated tagged histone HPV16 PsVs, including H2A, H2Ax, H2B, H3, H4, containing epitope-tagged 3xFLAG-thrombin-HA (3XFTHA) on the C terminus of histones (3XFTHA tagged histones). Beside core histones, we also specially look into H2Ax which is a member of H2A family and function in response to DNA damage response and

repair[43]. Moreover, we generated tagged L2 HPV16 PsV that serves as a control group, and this PsV contains the s3XFTHA tag fused to the C terminus of the L2 protein.

All PsVs have a relative low abundance of L2 but a very high levels of L1 on the Coomassie gel, as expected. Purified tagged L2 and tagged histone PsVs have a comparable level to that of unmodified wild-type (WT) L2 (Fig 2B), and there were good levels of total PsV yield or reporter viral genome. Purified tagged histone PsVs contained high amount of tagged core histones (Fig 2C). We infected HaCaT keratinocytes with luciferase-expressing HPV16 PsVs at different multiplicities of infection (MOI). Normalized luciferase activity of the BSA standard was measured at 24h post-infection. The infectivity of the tagged L2 virus was slightly lower than that of WT HPV16. Infectivity of tagged H2A and H2Ax viruses had around 50% infectivity compared to that of WT HPV16. H2B had relatively less infectivity. In contrast, tagged H3 and H4 viruses were relatively low or non-infectious, for reasons unknown (Fig 2D).

Detection of 3XFTHA-tagged histone PsVs in infected HaCaT keratinocytes

To identify the presence of these tagged HPV16 PsVs in infected cells, we performed immunofluorescence labeling after cells were infected with 3XFTHA tagged L2 or histones viruses to observe tagged L2 and tagged histones in infected cells. Mock-infected cells had no detectable FLAG or L1 signal. Tagged L2 signal in HPV16-infected cells often colocalized with L1 signals at 8 h post-infection. Furthermore, tagged H2A, H2Ax, H2B, and H3 in HPV16-infected cells presented spotted signals, with partial overlap with L1 signals. On the other hand, tagged H4 HPV16-infected cells barely had detectable H4 signals, somewhat consistent with the lower abundance of packaged H4-3XFTHA (Fig 3 and Fig 2C).

3XFTHA-tagged H3 and H4 interfere luciferase expression

PsVs with tagged H3 and H4 exhibited severely impaired infectivity (Fig 2D), yet cells infected with H3-3xFTHA PsV contained abundant tagged H3 signal, a result that was quite unexpected given the lack of infectivity compared to viruses containing tagged H2a and H2b (Fig 3). In order to clarify if certain tagged histones viruses were interfering with luciferase gene expression, we cotransfected pGL3 plasmid and tagged histone plasmids, into 293TT cells, without other viral components. Tagged H2A, H2Ax, and H2B transfected 293TT cells have comparable luciferase expression with control cells. Conversely, tagged H3 and H4 transfected 293TT cells have significantly lower luciferase expression (Fig 4A). Tagged H3 transfected cells contain comparable amounts of tagged H2A, H2Ax, and H2B, but lower levels of tagged H4 (Fig 4B). On the other hand, all tagged histone transfected HaCaT cells did not block the expression of luciferase (Fig 4C). Based on the western blot, only tagged H4 transfected HaCaT cells showed low transfection efficiency (Fig 4D). This indicates that tagged H2A, H2Ax, and H2B did not block pGL3 expression. However, tagged H3 and H4 may somehow cause repression of luciferase expression from pGL3, for reasons currently unknown. More discussion on these puzzling findings are provided below.

Viral histones are able to traffic to the late endosome

Human papillomaviruses enter host cells via a clathrin-independent endocytic pathway. After internalization, viral particles are transported from early endosomes (EE) into late endosomes (LE) and multivesicular bodies (MVBs), which are prerequisites for capsid uncoating, disassembly, and segregation of L1 from L2/vDNA complex [33], [44]. In the post-endocytic HPV trafficking, the delivery of viral particles to LE/MVBs is the critical step in HPV early infection[45].

To investigate the transport of viral histones to LE in the post-endocytic HPV trafficking, we infected HaCaT cells with 3XFTHA-tagged histone PsVs for 8h before PFA fixation and immunofluorescence staining. In mock-infected cells, we only detected the CD63 signal, a marker for late endosomes. In PsVs-infected cells, as expected, we detected tagged L2 signals that colocalized with L1 signals and accumulate at the late endosome. Similarly, many tagged H2A, H2B, and H3 signals are present in the late endosome as well, and colocalize with L1 signals. Unfortunately, tagged H4-infected cells had barely detected H4 signals, but L1 signals were present and accumulated at the late endosome (Fig 5). This result demonstrates that tagged viral histones in HaCaT cells are able to transport to the late endosome with L1. The reason behind the inability to detect H4-3xFTHA histones is not known but could indicate that this epitope tag is inaccessible to antibodies at these stages on PsV infection (perhaps the epitope is blocked by L1 or other molecules).

Viral histones accumulate and localize at nuclear PML bodies

L2/vDNA complexes accumulat at the TGN until the beginning of mitosis. Then, the L2/vDNA complexes are transported into the nucleus where they accumulate at nuclear PML bodies at late times post-infection. Previous research suggested that PML bodies are involved in host antiviral defenses, but many viruses overcome these defenses by targeting PML bodies, inducing degradation, or remodeling of PML body components[46], [47]. HPV16 vDNA targeting to nuclear PML bodies is the critical step for establishment of HPV16 infection and early gene transcription[48].

To determine if the viral histones accumulated at nuclear PML bodies at 42h post-infection, we infected HaCaT cells with 3XFTHA-tagged histone PsVs prior to methanol fixation and immunofluorescence staining. Mock-infected cells only exhibited PML

labeling. The majority of tagged L2 in HPV16-infected cells displayed flecked nuclear fluorescence and was partially colocalized with nuclear PML bodies. Similarly, tagged H2A, H2Ax, H2B, H3, and H4 HPV16-infected cells had tagged histone signals that were present in the nucleus and were partly colocalized with nuclear PML bodies (Fig 6A). Quantification showed that all 3XFTHA-tagged histones PsVs displayed the increased colocalization of PML bodies at late times post-infection (Fig 6B). Also, we infected cells treated with γ-secretase (γ-sec) inhibitor compound E, which fails L2 protrusion and blocks L2/vDNA traffic to TGN, acting as a negative control. Due to γ-sec inhibitor treatment, tagged L2 or histones signals accumulate at the side of the nucleus (Fig 6C). Quantification showed that γ-sec inhibitor treatment caused blocked the colocalization between the HA-tagged H2A and H3 signals and the PML marker (Fig. 6B). These findings support that viral histones are associated with L2/vDNA complex and trafficking together to reach the nucleus.

Conclusion and Discussion

Packaged histones traffic along with L2/vDNA to reach PML bodies during HPV infection.

Histones play critical roles in epigenetic regulation either through the expression and incorporation of different histone variants into chromatin, or by modifying histone tails to regulate histone activity. In this work, we explored whether the packaged core histones of virions are trafficked to the nucleus along with the L2/vDNA complex during HPV16 early infection by producing 3XFTHA tagged histone PsVs.

All core histone-3XFTHA pseudoviruses composed of L1/L2 capsid protein, 3XFTHA tagged histones, and pGL3 pesudogenome, and most 3XFTHA tagged histone virions are infectious, except tagged H3 and H4 virions (Fig. 2D). However, immunofluorescence experiments revealed that tagged H3 signals were detectable inside the infected cell, in the proper locations along with L1 capsid and cellular markers (Figs 3,5,6). Packaged H4-3xFTHA was also detectable but to a lesser extent, and only in the PML localization experiment at late times post infection (Fig 6). Interestingly, both 3XFTHA-tagged histone H3 and H4 lead to a repressed state of luciferase gene expression. This surprising finding is discussed in more detail below.

After HPV enters the cell, HPV subcellular trafficking is dependent on L2 and cellular sorting factors that transport vDNA from the early endosome, the late endosome/ MVBs, to the TGN, then to reach the nucleus. Here, we investigated the transport of tagged cellular histones during HPV16 PsVs infection by immunofluorescence staining. Our results suggested that tagged histones traffic to the late endosome, also, and colocalized with L1, like tagged L2, at 8h post-infection (Fig. 5). Moreover, tagged histones and

tagged L2 traveled to and accumulated at PML bodies (Fig 6A). The PML colocalization of all tested viruses with 3XFTHA-tagged histones was blocked by treatment with γ-secretase inhibitor (Fig 6C). These results demonstrate that tagged viral histones are likely associated with the L2/vDNA complexes and traffic to the nucleus during HPV16 viral infection in a γ-secretase- and L2-dependent manner.

Troubleshooting for production of high levels of tagged histones in pseudoviruses.

Initially, tagged H4 viruses were produced by transfecting pseudogenome and capsid protein L1/L2 plasmids into a 293TT subclone that stably expresses H4-3xFTHA (Fig. S1A). However, tagged H4 HPV16 PsVs contained less amount of tagged H4 in western blot (Fig. S1B). Furthermore, immunofluorescence results showed abundant L1 signal but no HA-tagged or FLAG-tagged H4 signal in infected cells (Fig. S1C). As a result of not enough tagged histone being present in the PsV, we figured to increase the yield of tagged histone in PsV by transfecting with not only pseudogenome and capsid protein L1/L2 plasmids but also H4-3XFTHA plasmid into regular 293TT cell line (Fig 2A). Fortunately, transfected with extra pCIP-H4-3xFTHA plasmid results in much higher tagged histone levels in new H4-3XFTHA viruses (Fig.S1D). Moving forward, we determined to make all tagged histones PsVs using this triple transfection protocol to avoid poor encapsidation of tagged histones.

High pH PBS wash caused signal artifact on tagged histones HPV16-infected cells when doing immunofluorescence staining

Our standard immunofluorescence method for detecting intracellular virions, involves washing the coverslip with pH 10.8 PBS to remove excess viral particles bound to the cell surface and ECM and prevent the detection of unwanted extracellular signals before fixation. Although we successfully produced a high yield of tagged histone viruses, using

our standard method the tagged H4 signals seemed to be present above the nucleus rather than distributed inside the cell (Fig S2). Interestingly, immunofluorescence staining showed that infected cells with normal PBS wash did not display this artifact. Thus, it is possible that high pH PBS wash destroyed the viral capsid structure and allowed tagged histone to be released, and likely bound to unknown cell surface and ECM receptors.

In addition to their main functions in the nucleus, histones have been reported to function as damage-associated molecular patterns (DAMPs) and endogenous danger signals when released into the extracellular space by damaged cells or activated immune cells[49]–[51]. Extracellular histones are released from apoptotic or necrotic cells that trigger innate immunity by activating Toll-like receptors, especially TLR2 and TLR4, which exist on the plasma membrane[50], [52], [53]. Also, neutrophils make neutrophil extracellular traps (NET) to kill invading microorganisms, and at least one of the NET components is histones which may spread out of the cell at the site of infection to mediate inflammation by binding to, TLR2 and TLR4[50], [54], [55]. Besides perhaps interacting with TLRs, histones possibly bind to the heparan sulfate proteoglycans (HSPG). HSPGs are composed of a proteoglycan core protein and covalently attached heparan sulfate (HS) chains that provide a negative charge to HSPGs[56], [57]. On the other hand, histones are positively charged due to a high amount of positively charged amino acids like arginine and lysine. After tagged histones are released out by high pH PBS wash, the negative charge of HSPG may make itself an ideal candidate to interact with positively charged histones. More work is be needed to determine which receptor(s) are involved in binding to the tagged histones released from alkaline-disrupted virions.

Tagged H3 and H4 interfere with luciferase expression during infection

According to the infectivity experiments, tagged H3 and H4 PsVs were non-infectious

(Fig 2D). However, tagged H3 signal was detect inside the infected cell at 8h post-infection (Fig 3) and many tagged H3 and H4 signals presented in nucleus at late times post-infection (Fig 6A). Further, we utilized lipofectamine transfection of both pGL3 pseudogenome and tagged histone plasmid to confirm if tagged histones interfere with luciferase gene expression. pGL3 pseudogenome plasmid has the SV40 Ori (origin of replication), and utilizes the SV40 T Ag (helicase that recognizes this Ori) to initial DNA replication. 293TT cells express abundant SV40 T Ag, that enable robust replication of the transfected pGL3 plasmid, resulting in very high expression of luciferase. On the other hand, due to lack of SV40 T Ag in HaCaT cells, transfected pGL3 does not replicate, and expresses lower levels of luciferase. The luciferase experiment revealed that tagged H3 and H4 transfected 293TT cells had significantly lower luciferase expression, but only in the 293TT system where pGL3 plasmid DNA replicates (Fig 4A). It is interesting to note that 3XFTHA-tagged H3 and H4 transfected into 293TT cells may lead to reduced luciferase expression during infection.

Histone marks would affect the interaction between DNA and histones that cause active or repressed chromatin[58]. In general, naked transfected DNA becomes chromatinized within the cell after transfection, and then replicates if the proper machinery is present (SV40 Ori and T Ag helicase), potentially acquiring new histones and epigenetic marks after DNA replication. These replicated pGL3 plasmids are assembled into infectious virus particles in the 293TT system. We speculate that packaged DNA with 3XFTHA-tagged H3 or H4 may have acquired different chromatinization and repressive histone marks after replication in 293TT cells. Then, pGL3 with this repressive chromatin may be packaged into virions, resulting in viruses that are non-infectious. Therefore, the further question is to investigate whether 3XFTHA-tagged H3 and H4 cause repressive marks only on replicated pGL3. We aim to follow up by looking to see if tagged H3 and

H4 affect pGL3 replication in the 293TT system, and to analyze the chromatin of H3- and H4-tagged viruses to see what kind of marks are present in their packaged chromatin, compared to infectious virions that contain L2-3XFTHA and H2a/H2b-3XFTHA.

Future studies of packaged histones

In summary, these studies describe the trafficking of viral histones in HPV early infection, demonstrating that viral histones may associate with L2/vDNA complex and are dependent on retrograde trafficking to reach the nucleus in HPV infection. Also, tagged histones H3 and H4 may alter the active chromatin of the luciferase gene to a repressed state. Our findings highlight the trafficking of packaged histones and the interaction between histone and vDNA and how that interaction may impact the viral DNA chromatin state and viral infectivity.

However, this study has limitation that will require further research. First, the study was limited to the colocalization of tagged L2 and cellular markers. We have not yet been able to examine tagged histones and L2 colocalization in the same cells during HPV16 infection. Additional studies are needed to confirm whether viral histones are actually associated with the L2/vDNA complex during infection. We generated PsVs that are able to detect and stain both L2 capsid protein and histone protein. Then, we will detect both L2 and histone signals with cell markers for endosome, trans-Golgi network, or PML bodies.

Furthermore, another experiment can be conducted to observe living cells during infection by producing mNeonGreen(mNG)-tagged histone virions. The advantage of mNG is very bright fluorescence, high photostability, and fast maturation. Also, mNG can be fused to specific proteins to facilitate protein subcellular localization studies without

impairing the function of the tagged protein. These good characteristics make it a good candidate for studying the trafficking of histones in living cells[59], [60]. Additionally, tagged histones partially colocalized with PML bodies, but their interactions are unclear. We plan to generate UltraID-tagged histones virions to explore the interaction between viral histones and PML bodies by proximity-dependent biotinylation. UltraID is the smallest and most highly efficient promiscuous biotin ligase, and it can convert biotin and ATP to Biotin-5'-AMP (reactive intermediate) that will react with lysine side chains on proximal protein to biotinylated. [61], [62].

Last but not least, I am curious about the role of histone modification correlated to early gene and late gene expression during the HPV life cycle. Isolate wild-type and mutant (E6 or E7) HPV minichromosome from infected cells at different times post-infection, then subject them to chromatin immunoprecipitation with specific antibodies which target modified histones to analyze and investigate the presence of acetylated or methylated site may reflect gene regulation during infection.

A.

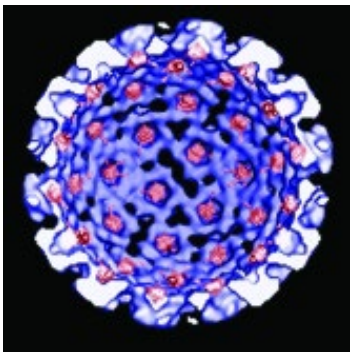

B.

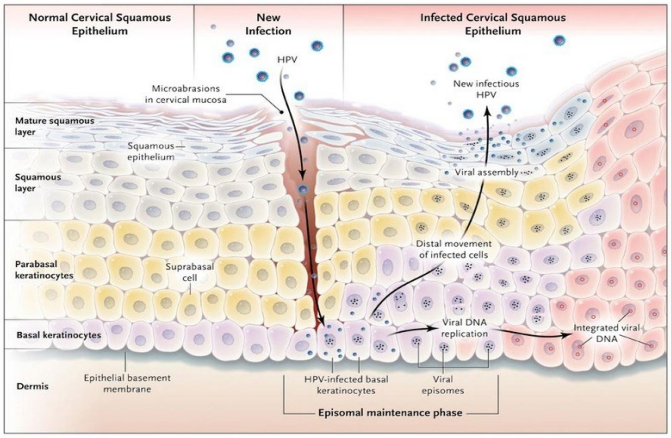
Normal Cervical Squamous Epithelium
New Infection
Infected Cervical Squamous Epithelium
HPV
Microabrasions in cervical mucosa
New infectious HPV
Mature squamous layer
Squamous epithelium
Squamous layer
Viral assembly
Distal movement of infected cells
Parabasal keratinocytes
Suprabasal cell
Basal keratinocytes
Viral DNA replication
Integrated viral DNA
Dermis
Epithelial basement membrane
HPV-infected basal keratinocytes
Viral episomes
Episomal maintenance phase

C.

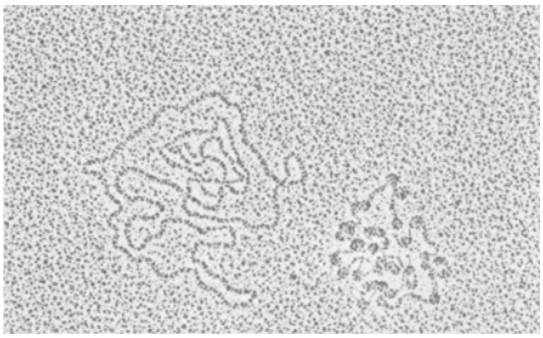

D.

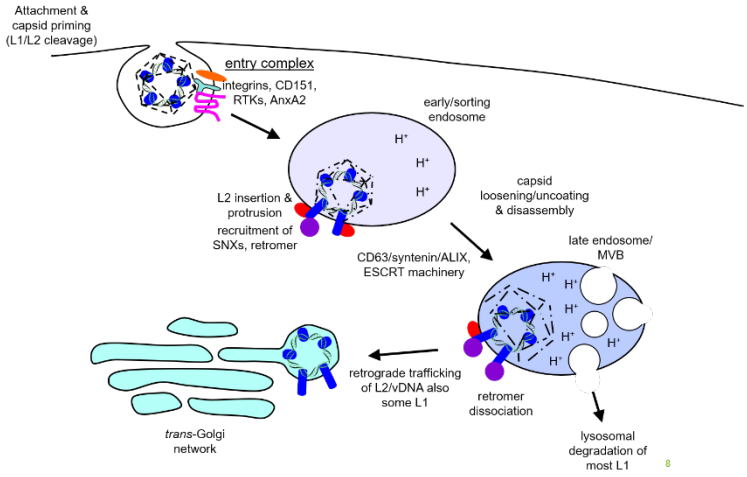
Attachment & capsid priming (L1/L2 cleavage)
entry complex
integrins, CD151, RTKs, AnxA2
early/sorting endosome
H+
L2 insertion & protrusion
recruitment of SNXs, retromer
capsid loosening/uncoating & disassembly
late endosome/ MVB
CD63/syntenin/ALIX, ESCRT machinery
retrograde trafficking of L2/vDNA also some L1
retromer dissociation
lysosomal degradation of most L1
trans-Golgi network

E.

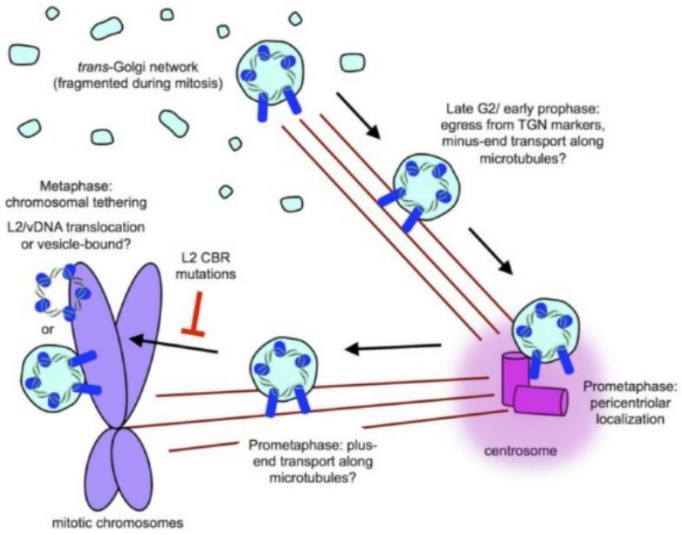
trans-Golgi network (fragmented during mitosis)
Late G2/ early prophase: egress from TGN markers, minus-end transport along microtubules?
Metaphase: chromosomal tethering
L2/vDNA translocation or vesicle-bound?
L2 CBR mutations
or
Prometaphase: pericentriolar localization
centrosome
Prometaphase: plus-end transport along microtubules?
mitotic chromosomes

Figure 1. Virology, pathogenesis and subcellular trafficking of HPV16

A. Structure of HPV16. HPV is comprised of major capsid protein L1 (blue), minor capsid protein L2(red), and viral histones associated with viral genome (not shown). Figure from [6]. **B. Pathogenesis of HPV16.** Infection of HPV16 requires access to the basal layer of stratified squamous epithelium. The viral genome maintains low copy number in basal keratinocytes. Infected cells start uncontrolled cellular division, followed by infected basal keratinocytes moving toward the upper layer of the cervical epithelium tissue that may develop cancers. The viral particles assembly and package in squamous layer and infectious HPV is released. Figure from [63]. **C. Electron micrographs of HPV nucleoprotein complexes.** HPV genomes are packaged with host histones, and are similar to the chromatin-like structure of host nuclear DNA. Figure from[7]. **D. Subcellular trafficking of HPV16: Interphase.** After binding to the entry complex, HPV enter the cell and traffics through the endosomal pathway. L2 capsid protein changes conformation to form the protrusion structure and act as an inducible transmembrane protein to help vDNA traffic to the TGN. The majority of L1 capsid protein segregates from L2/vDNA and is degrade in late endosomes/lysosomes. **E. Subcellular trafficking of HPV16: Mitosis.** While starting mitosis, the TGN naturally becomes fragmented and vesiculated, and L2/vDNA trafficks to chromosomes via microtubules. Figure from[42].

A.

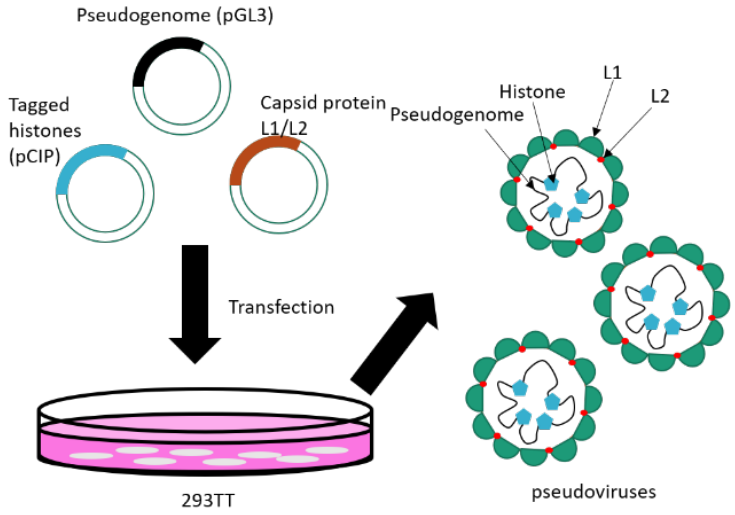
Pseudogenome (pGL3)
Tagged histones (pCIP)
Capsid protein L1/L2
Transfection
293TT
Histone
Pseudogenome
L1
L2
pseudoviruses

B.

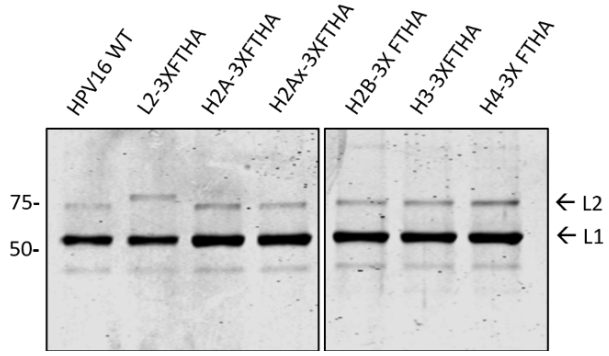
HPV16 WT
L2-3XFTHA
H2A-3XFTHA
H2Ax-3XFTHA
H2B-3X FTHA
H3-3XFTHA
H4-3X FTHA
75-
50-
L2
L1

C.

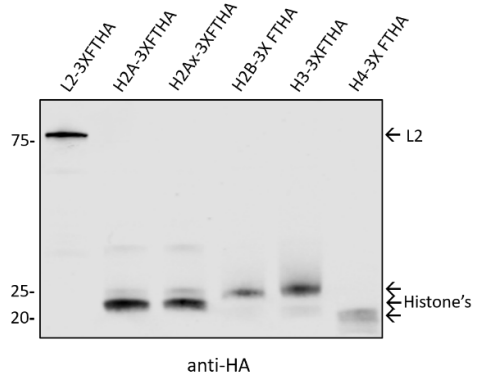
L2-3XFTHA
H2A-3XFTHA
H2Ax-3XFTHA
H2B-3X FTHA
H3-3XFTHA
H4-3X FTHA
75-
25-
20-
L2
Histone's
anti-HA

D.

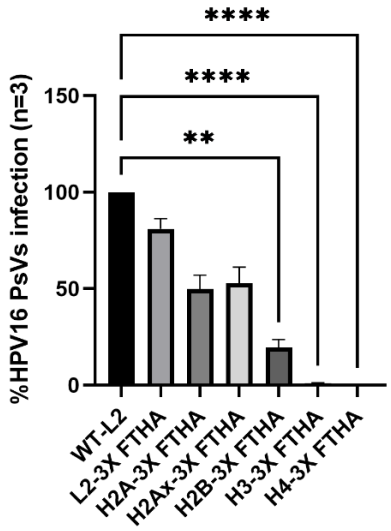
%HPV16 PsVs infection (n=3)
150
100
50
0
****
****
**
WT-L2
L2-3X FTHA
H2A-3X FTHA
H2Ax-3X FTHA
H2B-3X FTHA
H3-3X FTHA
H4-3X FTHA

Figure 2. Characterization of 3XFTHA tagged histone PsV

A. Schematic of pseudovirus production assay. Transfection of viral capsid proteins, tagged histones, and pseudogenome (Luciferase reporter gene) into 293TT cells to produce HPV-like viral particles. **B. Coomassie staining** of CsCl-purified tagged L2 and histones virions, compared to WT HPV16. Molecular weights are shown in kilodaltons. **C. Western blot** of CsCl-purified tagged histones virions, compared to L2-3XFTHA. Tagged L2 and histones were detected with rat anti-HA monoclonal antibody. Molecular weights are shown in kilodaltons. **D. Infection assay.** Relative infectivity of WT, tagged L2, and tagged histones viruses in HaCaT cells at an equal MOI, expressed relative to WT-L2, which is set at 100%. All infection values represent mean percent infection (±SEM, n = 3). p-values were calculated with one-way ANOVA (** $p < 0.01$ and **** $p < 0.0001$).

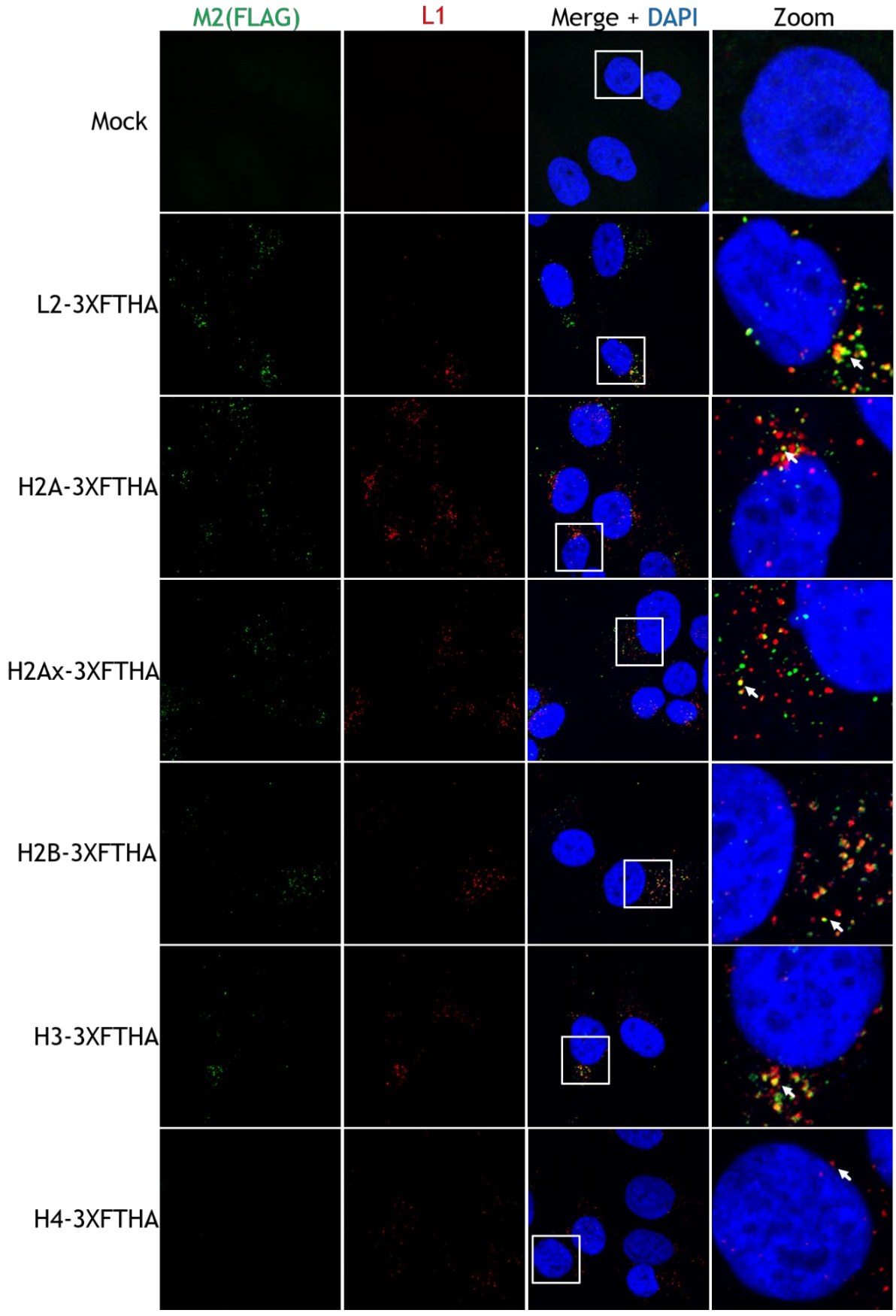
M2(FLAG)
L1
Merge + DAPI
Zoom
Mock
L2-3XFTHA
H2A-3XFTHA
H2Ax-3XFTHA
H2B-3XFTHA
H3-3XFTHA
H4-3XFTHA

Figure 3. Detection of tagged histone PsVs/ in infected HaCaT keratinocytes

Representative image slices (0.35 um thick) of HaCaT cells infected with WT L2-3XFTHA, H2A-3XFTHA, H2Ax-3XFTHA, H2B-3XFTHA, H3-3XFTHA, H4-3XFTHA PsV for 8 h. Tagged L2 and tagged histones were stained with FLAG (green), L1 was stained with the HPV16 polyclonal antibody (red), and nuclei were stained with DAPI (blue).

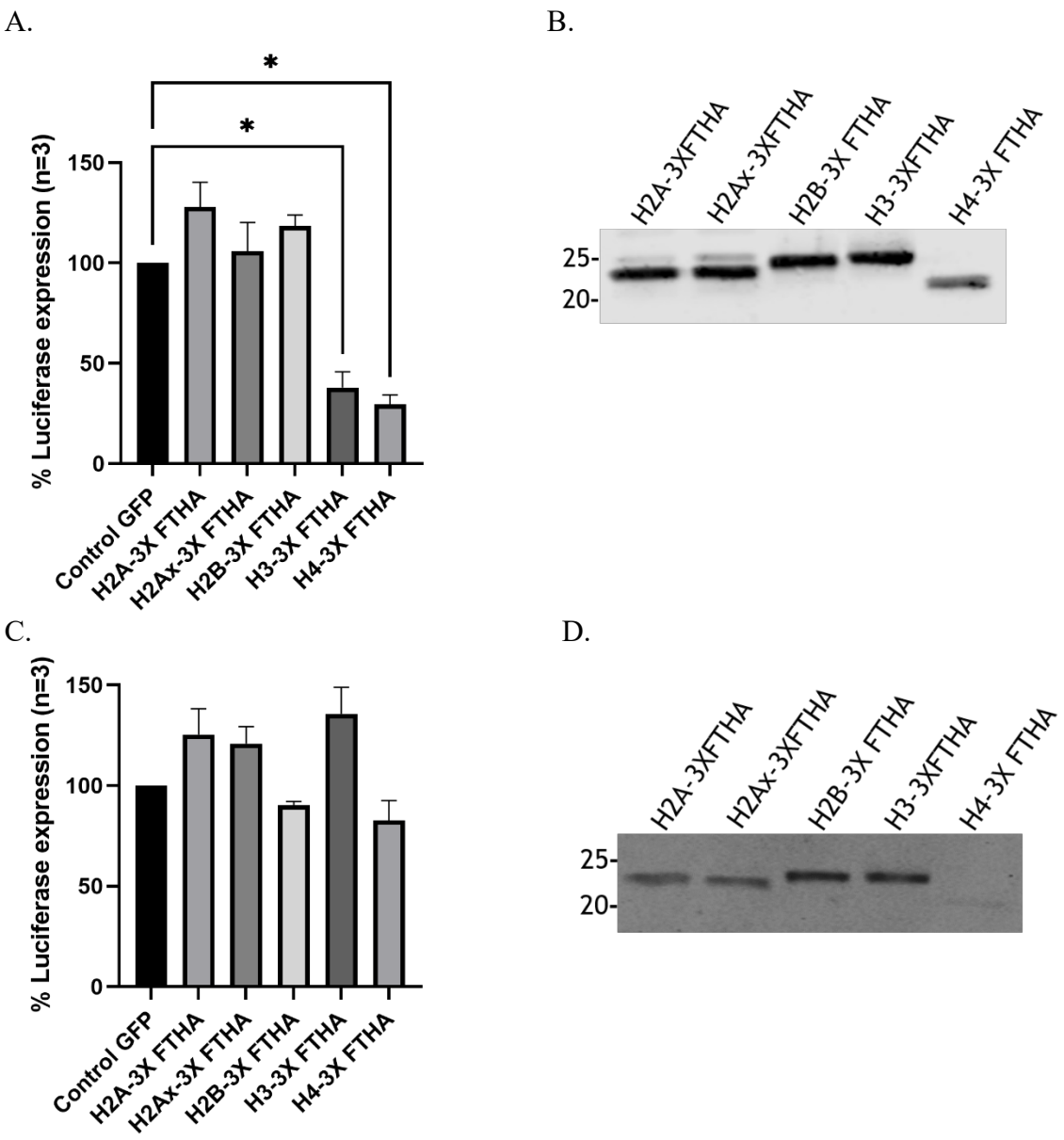

Figure 4. 3XFTHA-tagged H3 and H4 interfere with luciferase expression

A. Luciferase assay. Relative LUC activity of tagged histone transfected 293TT cells at an equal MOI, expressed relative to control cells, which is set at 100%. All values represent mean percent luciferase activity (±SEM, n = 3). p-values were calculated with one-way ANOVA (* $p < 0.05$). **B. Western blot** of tagged histone-transfected to 293TT cells. Tagged L2 and histones were detected with rat anti-HA monoclonal antibody. Molecular weights are shown in kilodaltons. **C. Luciferase assay.** Relative LUC activity of tagged histone transfection 293TT cells at an equal MOI, expressed relative to control cells, which is set at 100%. All values represent mean percent infection (±SEM, n = 3). p-values were calculated with one-way ANOVA. **D. Western blot** of tagged histones transfected to 293TT cells. Tagged L2 and histones were detected with rat anti-HA monoclonal antibody. Molecular weights are shown in kilodaltons.

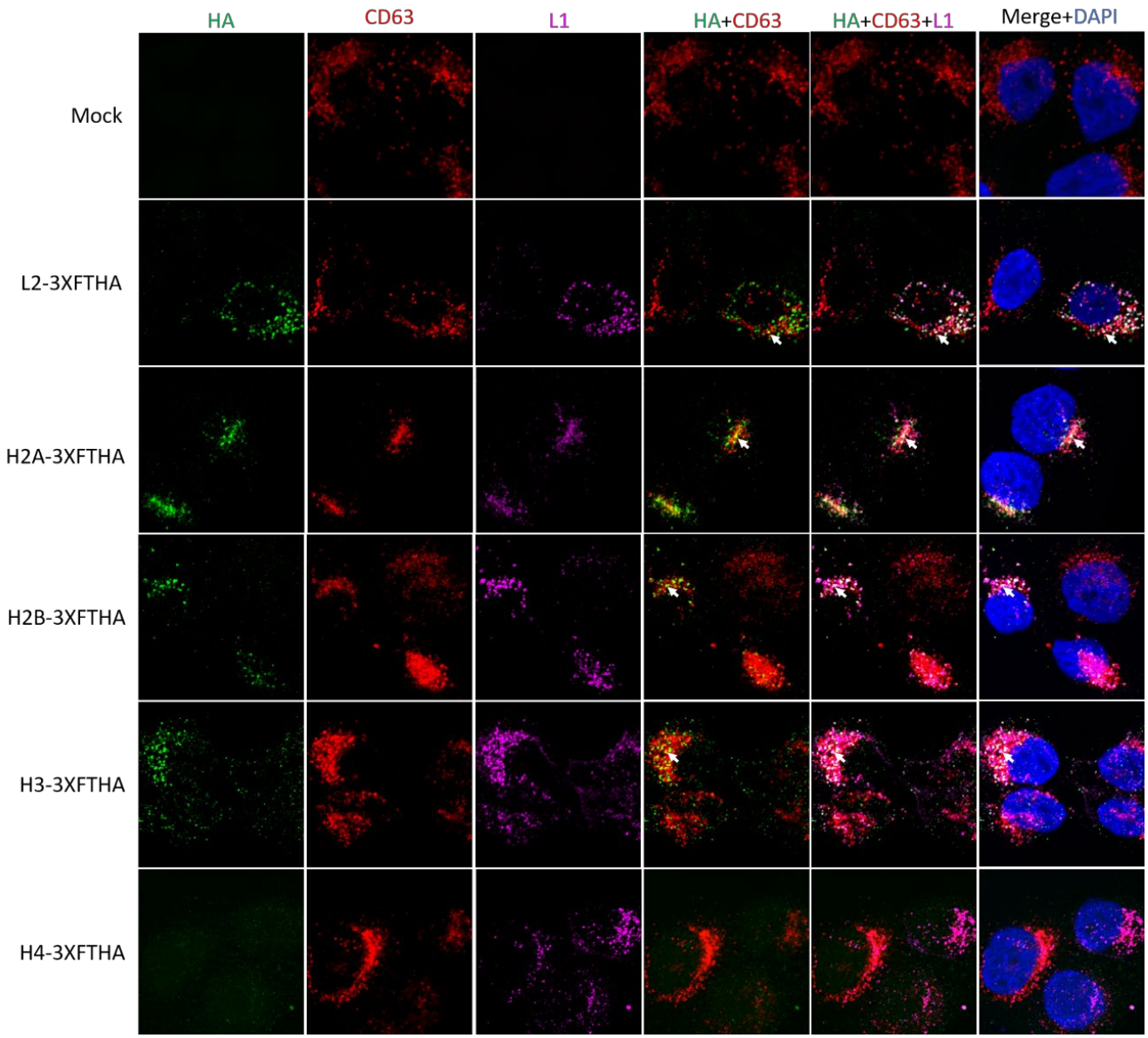

Figure 5. Viral histones are able to traffic to the late endosome

Representative image slices (0.25 um thick) of tagged histones HPV16-infected cells. HaCaT cells infected with WT L2-3XFTHA, H2A-3XFTHA, H2B-3XFTHA, H3-3XFTHA, H4-3XFTHA PsV. 8h post-infection, cells were fixed, permeabilized, and incubated with anti-HA antibody for tagged L2 and tagged histones(green), anti-CD63 antibody for late endosome (red), HPV16 polyclonal antibody for L1 (magenta), and DAPI to visualize nuclei (blue). White arrows show the colocalization signals.

A.

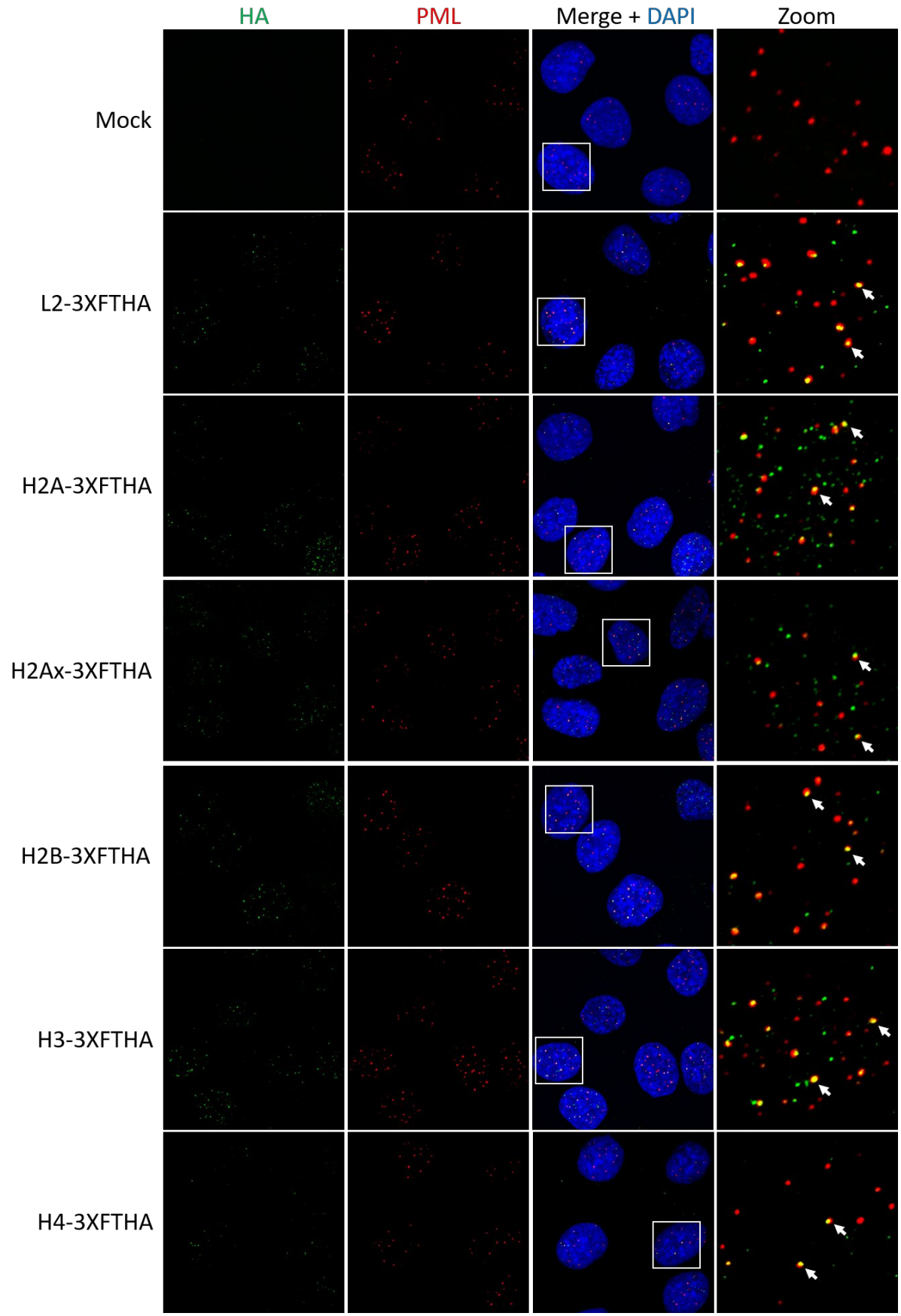
HA
PML
Merge + DAPI
Zoom
Mock
L2-3XFTHA
H2A-3XFTHA
H2Ax-3XFTHA
H2B-3XFTHA
H3-3XFTHA
H4-3XFTHA

B.

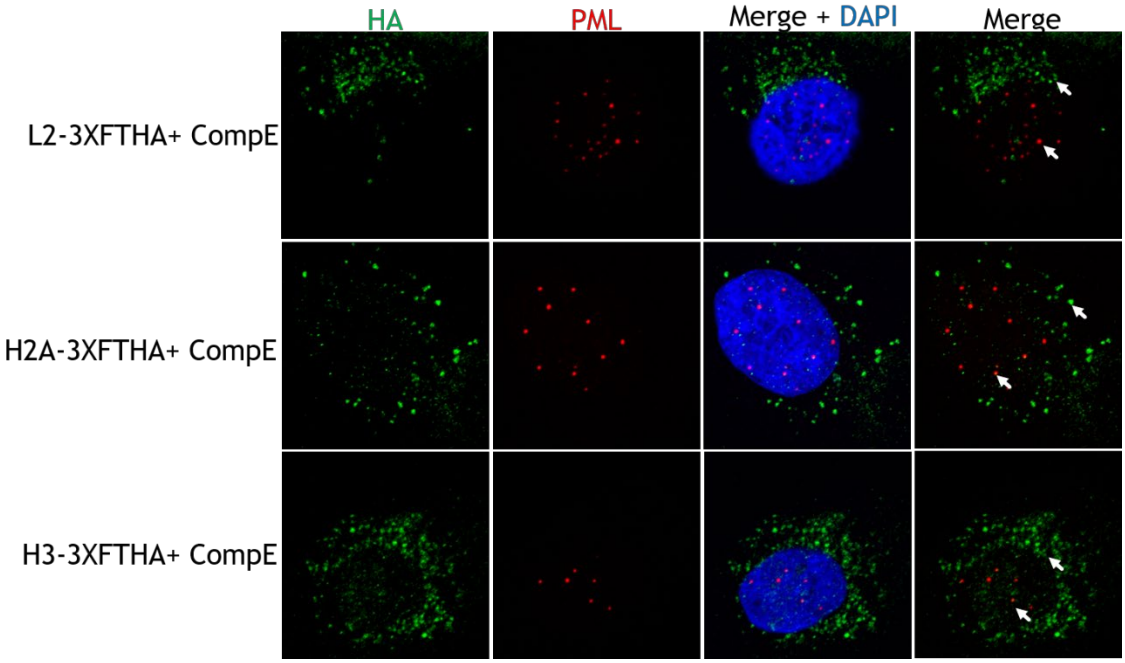

C.

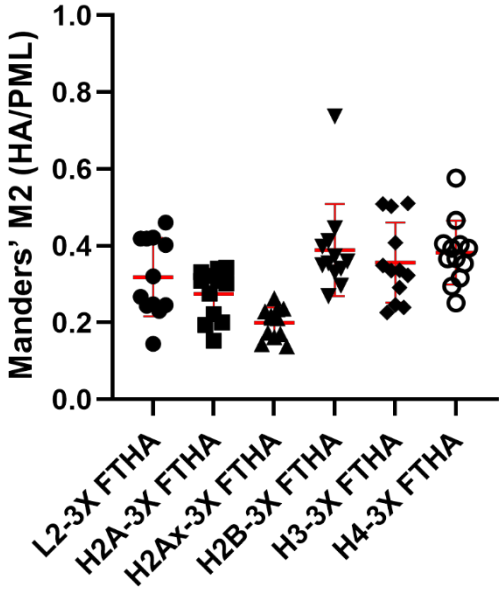

D.

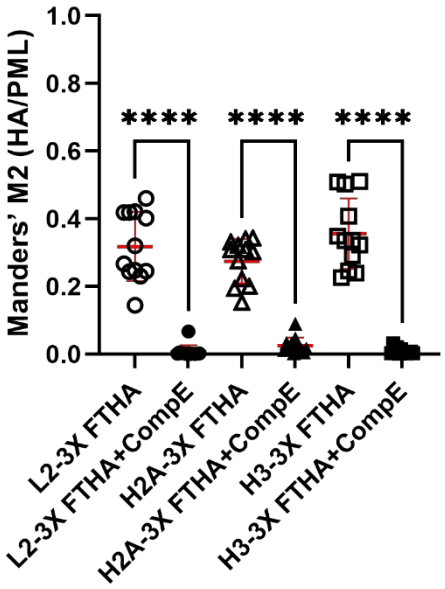

Figure 6. Viral histones localized at nuclear PML bodies

A. Representative image. HaCaT cells were infected with L2-3XFTHA, H2A-3XFTHA, H2Ax-3XFTHA, H2B-3XFTHA, H3-3XFTHA, H4-3XFTHA PsV for 18h. After 18 h infection, medium was changed, and infected cells were cultured an additional 24 h before methanol fixation and immunofluorescence staining. Tagged L2 and tagged histones were stained with rat anti-HA (green), nuclear PML bodies stained with ms anti-PML (red), and DAPI to visualize with nuclei (blue). Individual channels and the merged images are representative image slices (0.25 μm). **B. Representative**

image. HaCaT cells were infected with L2-3XFTHA, H2A-3XFTHA, H3-3XFTHAP sV with or without Compound E for 18h. After 18 h infection, medium was changed, and infected cells with or without Compound E treatment were cultured an additional 24 h before methanol fixation and immunofluorescence staining. Tagged L2 and tagged histones were stained with rat anti-HA (green), nuclear PML bodies stained with ms anti-PML (red), and DAPI to visualize with nuclei (blue). Individual channels and the merged images are representative image slices (0.25 μm). **C. Colocalization analysis** using the JACoP plugin of ImageJ. Manders colocalization coefficients were measured between HA:PML for multiple Z-stacks. The mean Manders coefficient and ±SEM were shown in red bars, each dot represents one cell/field. **D. Colocalization analysis** of 3XFTHA-tagged viruses with or without Compound E treatment using the JACoP plugin of ImageJ. Manders colocalization coefficients were measured between HA:PML for multiple Z-stacks. The mean Manders coefficient and ±SEM were shown in red bars, each dot represents one cell/field.

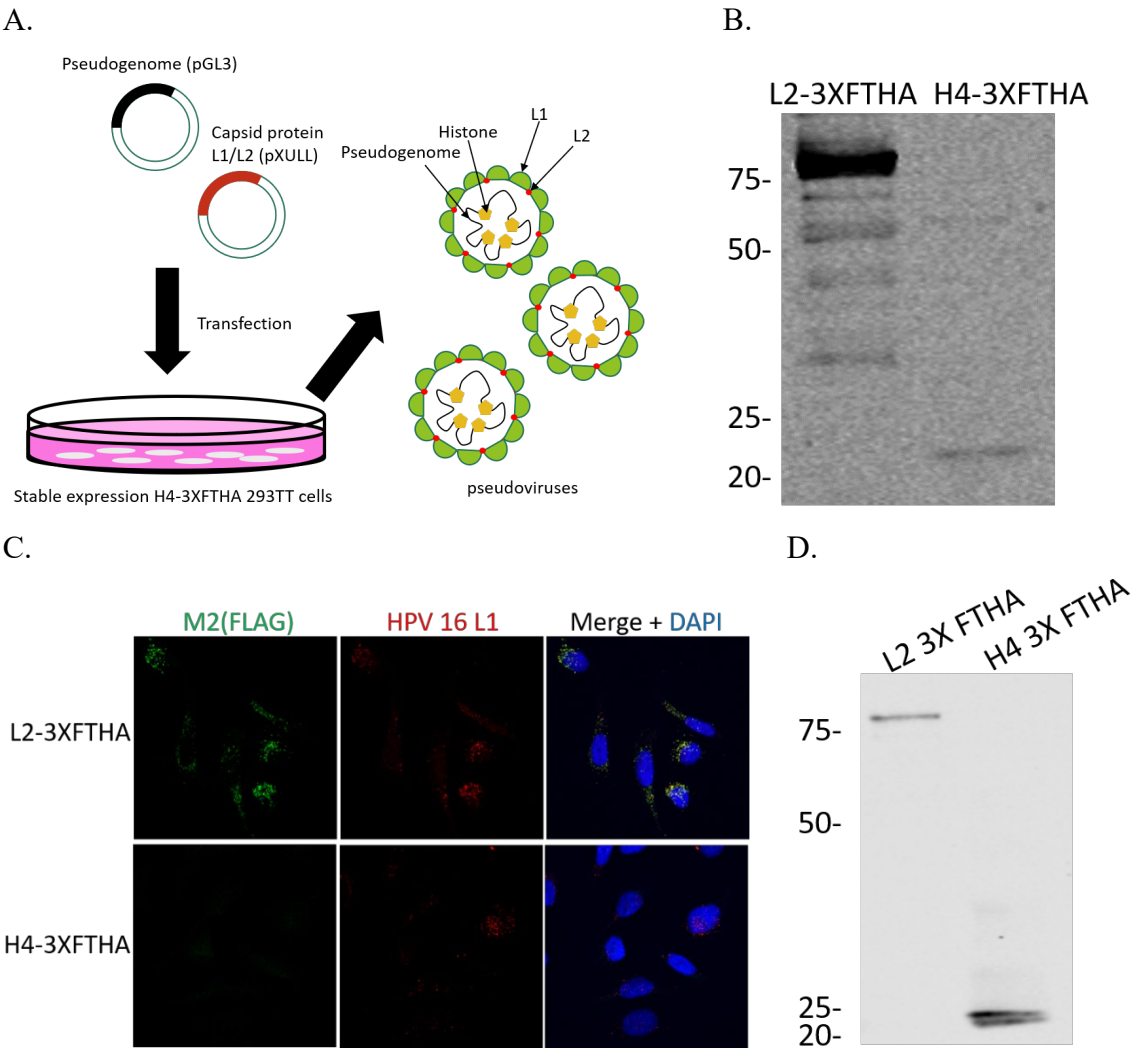

Figure S1. Troubleshooting for tagged histones PsVs production

A. Schematic of pseudovirus production assay. Transfection of viral capsid proteins and pseudogenome (luciferase reporter gene) into the stable expression of H4-3XFTHA 293TT cells to produce HPV-like viral particles. **B. Western Blot** of CsCl-purified tagged histone H4 virions showed a low level of tagged H4, compared to L2-3XFTHA. Tagged L2 and H4 were detected with rat anti-HA monoclonal antibody. Molecular weights are shown in kilodaltons. **C. Immunofluorescence** of tagged L2 and tagged H4 HPV16-infected cells. Tagged H4 signals are barely detected. Tagged L2 and tagged histones were stained with FLAG (green), L1 was stained with the HPV16 polyclonal antibody (red), and nuclei were stained with DAPI (blue).

D. Western Blot of CsCl-purified tagged histone H4 virions showed a high level of tagged H4, compared to L2-3XFTHA. Tagged L2 and H4 were detected with rat anti-HA monoclonal antibody. Molecular weights are shown in kilodaltons.

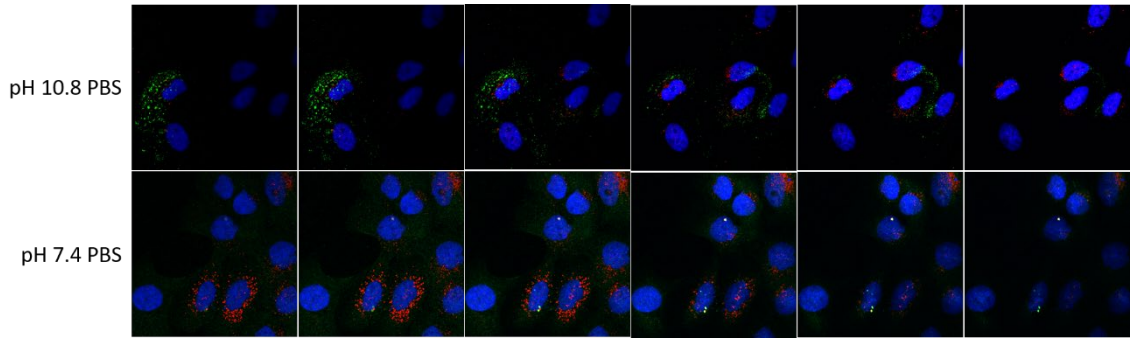

Figure S2. High pH PBS wash causes signal artifact in IF

Representative image slices (0.35 um thick) of HaCaT cells infected with H4-3XFTHA PsV for 8 h before pH10.8 or pH7.4 PBS wash, fixation, and immunofluorescence staining. Tagged H4 was stained with FLAG (green), L1 was stained with the HPV16 polyclonal antibody (red), and nuclei were stained with DAPI (blue).

References

[1] J. Doorbar *et al.*, "The biology and life-cycle of human papillomaviruses," *Vaccine*, vol. 30 Suppl 5, pp. F55-70, Nov. 2012, doi: 10.1016/j.vaccine.2012.06.083.

[2] N. Egawa, K. Egawa, H. Griffin, and J. Doorbar, "Human Papillomaviruses; Epithelial Tropisms, and the Development of Neoplasia," *Viruses*, vol. 7, no. 7, pp. 3863–3890, Jul. 2015, doi: 10.3390/v7072802.

[3] S. Ramakrishnan, S. Partricia, and G. Mathan, "Overview of high-risk HPV's 16 and 18 infected cervical cancer: pathogenesis to prevention," *Biomed Pharmacother*, vol. 70, pp. 103–110, Mar. 2015, doi: 10.1016/j.biopha.2014.12.041.

[4] H.-U. Bernard, R. D. Burk, Z. Chen, K. van Doorslaer, H. zur Hausen, and E.-M. de Villiers, "Classification of papillomaviruses (PVs) based on 189 PV types and proposal of taxonomic amendments," *Virology*, vol. 401, no. 1, pp. 70–79, May 2010, doi: 10.1016/j.virol.2010.02.002.

[5] E. F. Harding, A. G. Russo, G. J. H. Yan, L. K. Mercer, and P. A. White, "Revealing the uncharacterised diversity of amphibian and reptile viruses," *ISME Commun*, vol. 2, p. 95, Oct. 2022, doi: 10.1038/s43705-022-00180-x.

[6] C. B. Buck *et al.*, "Arrangement of L2 within the papillomavirus capsid," *J Virol*, vol. 82, no. 11, pp. 5190–5197, Jun. 2008, doi: 10.1128/JVI.02726-07.

[7] M. Favre, F. Breitburd, O. Croissant, and G. Orth, "Chromatin-like structures obtained after alkaline disruption of bovine and human papillomaviruses," *J Virol*, vol. 21, no. 3, pp. 1205–1209, Mar. 1977, doi: 10.1128/JVI.21.3.1205-1209.1977.

[8] E.-M. de Villiers, C. Fauquet, T. R. Broker, H.-U. Bernard, and H. zur Hausen, "Classification of papillomaviruses," *Virology*, vol. 324, no. 1, pp. 17–27, Jun. 2004, doi: 10.1016/j.virol.2004.03.033.

[9] K. L. Chua and A. Hjerpe, "Persistence of human papillomavirus (HPV) infections preceding cervical carcinoma," *Cancer*, vol. 77, no. 1, pp. 121–127, Jan. 1996, doi: 10.1002/(SICI)1097-0142(19960101)77:1<121::AID-CNCR20>3.0.CO;2-6.

[10] J. Doorbar, "The papillomavirus life cycle," *Journal of Clinical Virology*, vol. 32, pp. 7–15, Mar. 2005, doi: 10.1016/j.jcv.2004.12.006.

[11] C. B. J. Woodman, S. I. Collins, and L. S. Young, "The natural history of cervical HPV infection: unresolved issues," *Nat Rev Cancer*, vol. 7, no. 1, pp. 11–22, Jan. 2007, doi: 10.1038/nrc2050.

[12] F. Fehrmann and L. A. Laimins, "Human papillomaviruses: targeting differentiating epithelial cells for malignant transformation," *Oncogene*, vol. 22, no. 33, pp. 5201–5207, Aug. 2003, doi: 10.1038/sj.onc.1206554.

[13] M. Scheffner, B. A. Werness, J. M. Huibregtse, A. J. Levine, and P. M. Howley,

"The E6 oncoprotein encoded by human papillomavirus types 16 and 18 promotes the degradation of p53," *Cell*, vol. 63, no. 6, pp. 1129–1136, Dec. 1990, doi: 10.1016/0092-8674(90)90409-8.

[14] A. J. Klingelhutz, S. A. Foster, and J. K. McDougall, "Telomerase activation by the E6 gene product of human papillomavirus type 16," *Nature*, vol. 380, no. 6569, pp. 79–82, Mar. 1996, doi: 10.1038/380079a0.

[15] S. Chellappan *et al.*, "Adenovirus E1A, simian virus 40 tumor antigen, and human papillomavirus E7 protein share the capacity to disrupt the interaction between transcription factor E2F and the retinoblastoma gene product," *Proc Natl Acad Sci U S A*, vol. 89, no. 10, pp. 4549–4553, May 1992, doi: 10.1073/pnas.89.10.4549.

[16] A. J. Bannister and T. Kouzarides, "Regulation of chromatin by histone modifications," *Cell Res*, vol. 21, no. 3, pp. 381–395, Mar. 2011, doi: 10.1038/cr.2011.22.

[17] K. Ahmad and S. Henikoff, "Histone H3 variants specify modes of chromatin assembly," *Proc Natl Acad Sci U S A*, vol. 99 Suppl 4, no. Suppl 4, pp. 16477–16484, Dec. 2002, doi: 10.1073/pnas.172403699.

[18] C. L. Peterson and M.-A. Laniel, "Histones and histone modifications," *Current Biology*, vol. 14, no. 14, pp. R546–R551, Jul. 2004, doi: 10.1016/j.cub.2004.07.007.

[19] M. J. Fedor and E. Daniell, "Acetylation of histone-like proteins of adenovirus type 5," *J Virol*, vol. 35, no. 3, pp. 637–643, Sep. 1980, doi: 10.1128/JVI.35.3.637-643.1980.

[20] D. C. Avgousti, A. N. Della Fera, C. J. Otter, C. Herrmann, N. J. Pancholi, and M. D. Weitzman, "Adenovirus Core Protein VII Downregulates the DNA Damage Response on the Host Genome," *J Virol*, vol. 91, no. 20, pp. e01089-17, Oct. 2017, doi: 10.1128/JVI.01089-17.

[21] K. L. Lynch *et al.*, "A viral histone-like protein exploits antagonism between linker histones and HMGB proteins to obstruct the cell cycle," *Curr Biol*, vol. 31, no. 23, pp. 5227-5237.e7, Dec. 2021, doi: 10.1016/j.cub.2021.09.050.

[22] D. M. Pett, M. K. Estes, and J. S. Pagano, "Structural proteins of simian virus 40. I. Histone characteristics of low-molecular-weight polypeptides," *J Virol*, vol. 15, no. 2, pp. 379–385, Feb. 1975, doi: 10.1128/JVI.15.2.379-385.1975.

[23] B. Milavetz, L. Kallestad, A. Gefroh, N. Adams, E. Woods, and L. Balakrishnan, "Virion-mediated transfer of SV40 epigenetic information," *Epigenetics*, vol. 7, no. 6, pp. 528–534, Jun. 2012, doi: 10.4161/epi.20057.

[24] T. Enomoto, I. Kukimoto, M. Kawano, Y. Yamaguchi, A. J. Berk, and H. Handa, "In vitro reconstitution of SV40 particles that are composed of VP1/2/3 capsid proteins and nucleosomal DNA and direct efficient gene transfer," *Virology*, vol. 420, no. 1, pp. 1–9, Nov. 2011, doi: 10.1016/j.virol.2011.08.014.

[25] S. S. Porter *et al.*, “Histone Modifications in Papillomavirus Virion Minichromosomes,” *mBio*, vol. 12, no. 1, pp. e03274-20, Feb. 2021, doi: 10.1128/mBio.03274-20.

[26] T. Giroglou, L. Florin, F. Schäfer, R. E. Streeck, and M. Sapp, “Human papillomavirus infection requires cell surface heparan sulfate,” *J Virol*, vol. 75, no. 3, pp. 1565–1570, Feb. 2001, doi: 10.1128/JVI.75.3.1565-1570.2001.

[27] C. Cerqueira, P. Samperio Ventayol, C. Vogeley, and M. Schelhaas, “Kallikrein-8 Proteolytically Processes Human Papillomaviruses in the Extracellular Space To Facilitate Entry into Host Cells,” *J Virol*, vol. 89, no. 14, pp. 7038–7052, Jul. 2015, doi: 10.1128/JVI.00234-15.

[28] K. F. Richards, M. Bienkowska-Haba, J. Dasgupta, X. S. Chen, and M. Sapp, “Multiple heparan sulfate binding site engagements are required for the infectious entry of human papillomavirus type 16,” *J Virol*, vol. 87, no. 21, pp. 11426–11437, Nov. 2013, doi: 10.1128/JVI.01721-13.

[29] A. Dziduszko and M. A. Ozbun, “Annexin A2 and S100A10 regulate human papillomavirus type 16 entry and intracellular trafficking in human keratinocytes,” *J Virol*, vol. 87, no. 13, pp. 7502–7515, Jul. 2013, doi: 10.1128/JVI.00519-13.

[30] M. Evander, I. H. Frazer, E. Payne, Y. M. Qi, K. Hengst, and N. A. McMillan, “Identification of the alpha6 integrin as a candidate receptor for papillomaviruses,” *J Virol*, vol. 71, no. 3, pp. 2449–2456, Mar. 1997, doi: 10.1128/JVI.71.3.2449-2456.1997.

[31] Z. Surviladze, A. Dziduszko, and M. A. Ozbun, “Essential roles for soluble virion-associated heparan sulfonated proteoglycans and growth factors in human papillomavirus infections,” *PLoS Pathog*, vol. 8, no. 2, p. e1002519, Feb. 2012, doi: 10.1371/journal.ppat.1002519.

[32] K. D. Scheffer *et al.*, “Tetraspanin CD151 mediates papillomavirus type 16 endocytosis,” *J Virol*, vol. 87, no. 6, pp. 3435–3446, Mar. 2013, doi: 10.1128/JVI.02906-12.

[33] M. Bienkowska-Haba, C. Williams, S. M. Kim, R. L. Garcea, and M. Sapp, “Cyclophilins facilitate dissociation of the human papillomavirus type 16 capsid protein L1 from the L2/DNA complex following virus entry,” *J Virol*, vol. 86, no. 18, pp. 9875–9887, Sep. 2012, doi: 10.1128/JVI.00980-12.

[34] R. M. Richards, D. R. Lowy, J. T. Schiller, and P. M. Day, “Cleavage of the papillomavirus minor capsid protein, L2, at a furin consensus site is necessary for infection,” *Proc Natl Acad Sci U S A*, vol. 103, no. 5, pp. 1522–1527, Jan. 2006, doi: 10.1073/pnas.0508815103.

[35] S. K. Campos, “Subcellular Trafficking of the Papillomavirus Genome during Initial Infection: The Remarkable Abilities of Minor Capsid Protein L2,” *Viruses*, vol. 9, no. 12, p. 370, Dec. 2017, doi: 10.3390/v9120370.

[36] M. Schelhaas *et al.*, “Entry of human papillomavirus type 16 by actin-dependent, clathrin- and lipid raft-independent endocytosis,” *PLoS Pathog*, vol. 8, no. 4, p. e1002657, 2012, doi: 10.1371/journal.ppat.1002657.

[37] N. Kämper *et al.*, “A membrane-destabilizing peptide in capsid protein L2 is required for egress of papillomavirus genomes from endosomes,” *J Virol*, vol. 80, no. 2, pp. 759–768, Jan. 2006, doi: 10.1128/JVI.80.2.759-768.2006.

[38] S. DiGiuseppe *et al.*, “Topography of the Human Papillomavirus Minor Capsid Protein L2 during Vesicular Trafficking of Infectious Entry,” *J Virol*, vol. 89, no. 20, pp. 10442–10452, Oct. 2015, doi: 10.1128/JVI.01588-15.

[39] M. P. Bronnimann, J. A. Chapman, C. K. Park, and S. K. Campos, “A transmembrane domain and GxxxG motifs within L2 are essential for papillomavirus infection,” *J Virol*, vol. 87, no. 1, pp. 464–473, Jan. 2013, doi: 10.1128/JVI.01539-12.

[40] W. Zhang, T. Kazakov, A. Popa, and D. DiMaio, “Vesicular trafficking of incoming human papillomavirus 16 to the Golgi apparatus and endoplasmic reticulum requires γ-secretase activity,” *mBio*, vol. 5, no. 5, pp. e01777-01714, Sep. 2014, doi: 10.1128/mBio.01777-14.

[41] P. M. Day, C. D. Thompson, R. M. Schowalter, D. R. Lowy, and J. T. Schiller, “Identification of a role for the trans-Golgi network in human papillomavirus 16 pseudovirus infection,” *J Virol*, vol. 87, no. 7, pp. 3862–3870, Apr. 2013, doi: 10.1128/JVI.03222-12.

[42] C. M. Calton *et al.*, “Translocation of the papillomavirus L2/vDNA complex across the limiting membrane requires the onset of mitosis,” *PLoS Pathog*, vol. 13, no. 5, p. e1006200, May 2017, doi: 10.1371/journal.ppat.1006200.

[43] J. Yuan, R. Adamski, and J. Chen, “Focus on histone variant H2AX: to be or not to be,” *FEBS Lett*, vol. 584, no. 17, pp. 3717–3724, Sep. 2010, doi: 10.1016/j.febslet.2010.05.021.

[44] K. H. Müller *et al.*, “Inhibition by Cellular Vacuolar ATPase Impairs Human Papillomavirus Uncoating and Infection,” *Antimicrob Agents Chemother*, vol. 58, no. 5, pp. 2905–2911, May 2014, doi: 10.1128/AAC.02284-13.

[45] L. Gräßel *et al.*, “The CD63-Syntenin-1 Complex Controls Post-Endocytic Trafficking of Oncogenic Human Papillomaviruses,” *Sci Rep*, vol. 6, p. 32337, Aug. 2016, doi: 10.1038/srep32337.

[46] “DNA viruses and viral proteins that interact with PML nuclear bodies | Oncogene.” https://www.nature.com/articles/1204759 (accessed May 31, 2023).

[47] R. D. Everett and M. K. Chelbi-Alix, “PML and PML nuclear bodies: Implications in antiviral defence,” *Biochimie*, vol. 89, no. 6, pp. 819–830, Jun. 2007, doi: 10.1016/j.biochi.2007.01.004.

[48] P. M. Day, C. C. Baker, D. R. Lowy, and J. T. Schiller, “Establishment of

papillomavirus infection is enhanced by promyelocytic leukemia protein (PML) expression," *Proc Natl Acad Sci U S A*, vol. 101, no. 39, pp. 14252–14257, Sep. 2004, doi: 10.1073/pnas.0404229101.

[49] J. Xu *et al.*, "Extracellular histones are major mediators of death in sepsis," *Nat Med*, vol. 15, no. 11, pp. 1318–1321, Nov. 2009, doi: 10.1038/nm.2053.

[50] R. Allam, S. V. R. Kumar, M. N. Darisipudi, and H.-J. Anders, "Extracellular histones in tissue injury and inflammation," *J Mol Med (Berl)*, vol. 92, no. 5, pp. 465–472, May 2014, doi: 10.1007/s00109-014-1148-z.

[51] R. Chen, R. Kang, X.-G. Fan, and D. Tang, "Release and activity of histone in diseases," *Cell Death Dis*, vol. 5, no. 8, p. e1370, Aug. 2014, doi: 10.1038/cddis.2014.337.

[52] J. Xu, X. Zhang, M. Monestier, N. L. Esmon, and C. T. Esmon, "Extracellular histones are mediators of death through TLR2 and TLR4 in mouse fatal liver injury," *J Immunol*, vol. 187, no. 5, pp. 2626–2631, Sep. 2011, doi: 10.4049/jimmunol.1003930.

[53] F. Semeraro *et al.*, "Extracellular histones promote thrombin generation through platelet-dependent mechanisms: involvement of platelet TLR2 and TLR4," *Blood*, vol. 118, no. 7, pp. 1952–1961, Aug. 2011, doi: 10.1182/blood-2011-03-343061.

[54] V. Brinkmann *et al.*, "Neutrophil extracellular traps kill bacteria," *Science*, vol. 303, no. 5663, pp. 1532–1535, Mar. 2004, doi: 10.1126/science.1092385.

[55] A. S. Wilson *et al.*, "Neutrophil extracellular traps and their histones promote Th17 cell differentiation directly via TLR2," *Nat Commun*, vol. 13, no. 1, p. 528, Jan. 2022, doi: 10.1038/s41467-022-28172-4.

[56] S. Sarrazin, W. C. Lamanna, and J. D. Esko, "Heparan Sulfate Proteoglycans," *Cold Spring Harb Perspect Biol*, vol. 3, no. 7, p. a004952, Jul. 2011, doi: 10.1101/cshperspect.a004952.

[57] M. D. Stewart and R. D. Sanderson, "Heparan sulfate in the nucleus and its control of cellular functions," *Matrix Biology*, vol. 35, pp. 56–59, Apr. 2014, doi: 10.1016/j.matbio.2013.10.009.

[58] T. Jenuwein and C. D. Allis, "Translating the Histone Code," *Science*, vol. 293, no. 5532, pp. 1074–1080, Aug. 2001, doi: 10.1126/science.1063127.

[59] N. C. Shaner *et al.*, "A bright monomeric green fluorescent protein derived from Branchiostoma lanceolatum," *Nat Methods*, vol. 10, no. 5, pp. 407–409, May 2013, doi: 10.1038/nmeth.2413.

[60] L. Hostettler, L. Grundy, S. Käser-Pébernard, C. Wicky, W. R. Schafer, and D. A. Glauser, "The Bright Fluorescent Protein mNeonGreen Facilitates Protein Expression Analysis In Vivo," *G3 Genes|Genomes|Genetics*, vol. 7, no. 2, pp. 607–615, Feb. 2017, doi: 10.1534/g3.116.038133.

[61] L. Kubitz *et al.*, "Engineering of ultraID, a compact and hyperactive enzyme for

proximity-dependent biotinylation in living cells," *Commun Biol*, vol. 5, no. 1, Art. no. 1, Jul. 2022, doi: 10.1038/s42003-022-03604-5.

[62] X. Zhao *et al.*, "ultraID: a compact and efficient enzyme for proximity-dependent biotinylation in living cells." bioRxiv, p. 2021.06.16.448656, Jun. 16, 2021. doi: 10.1101/2021.06.16.448656.

[63] J. A. Kahn, "HPV Vaccination for the Prevention of Cervical Intraepithelial Neoplasia," *N Engl J Med*, vol. 361, no. 3, pp. 271–278, Jul. 2009, doi: 10.1056/NEJMct0806938.

Wendy thesis version

Final Audit Report 2023-07-17

Created:	2023-07-17
By:	Nian Chi (nianyuchi@arizona.edu)
Status:	Signed
Transaction ID:	CBJCHBCAABAArp9HgMIAeGGhdkDeZDRjOn3V-o2G8QLq

"Wendy thesis version" History

Document created by Nian Chi (nianyuchi@arizona.edu)
2023-07-17 - 5:01:56 PM GMT

Document emailed to Samuel Campos (skcampos@arizona.edu) for signature
2023-07-17 - 5:13:28 PM GMT

Email viewed by Samuel Campos (skcampos@arizona.edu)
2023-07-17 - 5:18:58 PM GMT

Document e-signed by Samuel Campos (skcampos@arizona.edu)
Signature Date: 2023-07-17 - 5:19:52 PM GMT - Time Source: server

Document emailed to Lonnie Lybarger (lybarger@arizona.edu) for signature
2023-07-17 - 5:19:53 PM GMT

Email viewed by Lonnie Lybarger (lybarger@arizona.edu)
2023-07-17 - 6:13:29 PM GMT

Document e-signed by Lonnie Lybarger (lybarger@arizona.edu)
Signature Date: 2023-07-17 - 6:13:46 PM GMT - Time Source: server

Document emailed to Ritu Pandey (ritu@arizona.edu) for signature
2023-07-17 - 6:13:48 PM GMT

Email viewed by Ritu Pandey (ritu@arizona.edu)
2023-07-17 - 6:16:50 PM GMT

Document e-signed by Ritu Pandey (ritu@arizona.edu)
Signature Date: 2023-07-17 - 6:39:05 PM GMT - Time Source: server

Agreement completed.
2023-07-17 - 6:39:05 PM GMT